HHS Public Access

Author manuscript

Epilepsy Res. Author manuscript; available in PMC 2016 September 01.

Published in final edited form as:

Epilepsy Res. 2015 September ; 115: 45–54. doi:10.1016/j.eplepsyres.2015.05.005.

Effects of site-specific infusions of methionine sulfoximine on the temporal progression of seizures in a rat model of mesial temporal lobe epilepsy

Roni Dhaher[a], **Helen Wang**[a], **Shaun E Gruenbaum**[a], **Nathan Tu**[a], **Tih-Shih W Lee**[c], **Hitten P Zaveri**[b], and **Tore Eid**[a,*]

[a] Department of Laboratory Medicine, Yale School of Medicine, 330 Cedar St., PO Box 208083, New Haven, CT 06520-8035, USA

[b] Department of Neurology, Yale School of Medicine, New Haven, CT 06520, USA

[c] Department of Psychiatry Yale School of Medicine, New Haven, CT 06520, USA

SUMMARY

Glutamine synthetase (GS) in astrocytes is critical for metabolism of glutamate and ammonia in the brain, and perturbations in the anatomical distribution and activity of the enzyme are likely to adversely affect synaptic transmission. GS is deficient in discrete regions of the hippocampal formation in patients with mesial temporal lobe epilepsy (MTLE), a disorder characterized by brain glutamate excess and recurrent seizures. To investigate the role of site-specific inhibition of GS in MTLE, we chronically infused the GS inhibitor methionine sulfoximine (MSO) into one of the following areas of adult laboratory rats: (1) the angular bundle, $n = 6$; (2) the deep entorhinal cortex (EC), $n = 7$; (3) the stratum lacunosum-moleculare of CA1, $n = 7$; (4) the molecular layer of the subiculum, $n = 10$; (5) the hilus of the dentate gyrus, $n = 6$; and (6) the lateral ventricle, $n = 6$. Twelve animals were infused with phosphate buffered saline (PBS) into the same areas to serve as controls. All infusions were unilateral, and animals were monitored by continuous video-intracranial EEG recordings for 3 weeks to capture seizure activity. All animals infused with MSO into the entorhinal–hippocampal area exhibited recurrent seizures that were particularly frequent during the first 3 days of infusion and that continued to recur for the entire 3 week recording period. Only a fraction of animals infused with MSO into the lateral ventricle had recurrent seizures, which occurred at a lower frequency compared with the other MSO infused group. Infusion of MSO into the hilus of the dentate gyrus resulted in the highest total number of seizures over the 3-week recording period. Infusion of MSO into all brain regions studied, with the exception of the lateral ventricle, led to a change in the composition of seizure severity over time. Low-grade (stages 1–3) seizures were more prevalent early during infusion, while severe (stages 4–5) seizures were more prevalent later. Thus, the site of GS inhibition within the brain determines the pattern and temporal evolution of recurrent seizures in the MSO model of MTLE.

* Corresponding author. Tel.: +1 203 688 2635; fax: +1 203 688 8597. tore.eid@yale.edu (T. Eid)..

The authors have no conflicts of interest to declare.

Appendix A. Supplementary data

Supplementary data associated with this article can be found, in the online version, at http://dx.doi.org/10.1016/j.eplepsyres.2015.05.005

Keywords

Astrocytes; Glutamate; Glutamine synthetase; Metabolism; Plasticity

Introduction

Being the most abundant excitatory neurotransmitter in the brain, glutamate is critical for neuronal signaling in health and disease. Because slight elevations of extracellular brain glutamate levels can lead to excessive neurotransmission, seizures, and neuronal death (During and Spencer, 1993; Olney, 1978; Olney et al., 1972), several mechanisms are in place to maintain extracellular glutamate homeostasis. Two of the most important mechanisms are cellular uptake via glutamate transporters (Danbolt, 2001), and intracellular metabolism to less excitatory molecules, such as glutamine (Martinez-Hernandez et al., 1977).

We discovered that one of the key metabolizing enzymes of brain glutamate – glutamine synthetase (GS) – is deficient in astrocytes in humans with medication refractory mesial temporal lobe epilepsy (MTLE) (Eid et al., 2004; van der Hel et al., 2005). This deficiency was most pronounced in the surgically resected seizure focus of the brain, particularly in the CA1, CA3 and dentate gyrus of the hippocampal formation (Eid et al., 2004). We hypothesized that the loss of GS in MTLE would perturb the homeostasis of brain glutamate and lead to recurrent seizures.

To test our hypothesis we chronically inhibited GS in the hippocampal formation of normal laboratory rats, using continuous brain infusions of the GS inhibitor methionine sulfoximine (MSO). The MSO-infused rats developed increased concentrations of glutamate in hippocampal astrocytes (Perez et al., 2012), loss of hippocampal neurons and recurrent seizures (Eid et al., 2008; Wang et al., 2009), suggesting that a deficiency in GS is implicated in the pathophysiology of MTLE.

Alterations in brain GS mRNA, protein, and enzyme activity have been reported in several neurological and psychiatric conditions other than epilepsy, such as Alzheimer's disease (Robinson, 2001), glioblastoma (Rosati et al., 2009), schizophrenia (Bruneau et al., 2005), and major depressive disorder (Lee et al., 2013; Rajkowska and Stockmeier, 2013). Typical for these conditions, and for epilepsy, is that the GS alterations are not uniformly detected throughout the brain. In MTLE, the loss of GS is most pronounced in CA1, CA3 and the dentate hilus with relatively higher levels of the enzyme being present in the subiculum and adjacent neocortical structures (Eid et al., 2004). In patients with neocortical epilepsies, GS is deficient in the amygdala but not in the neocortical seizure focus (Steffens et al., 2005). In glioblastoma, the deficiency in GS is preferential to the tumor site (Rosati et al., 2009), and in Alzheimer's disease GS is aberrantly expressed in neurons within senile plaques (Robinson, 2001).

Due to the topographic differences in GS expression in multiple brain disorders, it is reasonable to postulate that microanatomical alterations of GS cause focal perturbations of glutamate homeostasis with network-specific effects on neurotransmission. Depending on

the neuronal network involved, such alterations may affect a variety of brain modalities. As a step toward understanding the functional consequences of network-specific alterations of GS in epilepsy, we inhibited GS in discrete areas of the entorhinal–hippocampal (Ent–Hip) circuit using stereotaxic brain infusions of MSO. We then assessed the effects on abnormal brain activity, particularly the frequency and severity of seizures over a continuous period of 3 weeks. Our decision to study the Ent–Hip circuit was based on the observations that GS is deficient in discrete areas of the circuit in MTLE (Eid et al., 2004), and that the Ent–Hip area is critical for initiation of seizures in this disorder (Spencer and Spencer, 1994). Because electrophysiological studies of humans with epilepsy and animal models have shown differential patterns of neuronal activity within the Ent–Hip network (Cohen et al., 2002; de Guzman et al., 2006; Pitkanen et al., 1995; Toyoda et al., 2013), we hypothesized that the anatomical site of MSO infusion would dictate the expression pattern of recurrent seizures.

Materials and methods

Chemicals and animals

All chemicals were purchased from Sigma Chemical Co. (St. Louis, MO.) unless otherwise noted. Male Sprague Dawley rats were obtained from Charles River Laboratories (Wilmington, MA.). Upon arrival, rats were housed in groups (2–3 rats/cage) and maintained in a temperature-controlled colony room (21–23 °C) on a 12 h light–dark cycle. Rats were allowed free access to food and water, and underwent at least 1 week of acclimation prior to surgery. All procedures were approved by the Institutional Animal Care and Use Committee at Yale University and were conducted in accordance with current guidelines.

Surgery

Rats (330–400 g) were anesthetized with 0.5% to 2% Isoflurane (Baxter, Deerfield, IL) in O_2 and placed in a stereotaxic frame (David Kopf Instruments, Tujunga, CA). A 30-ga stainless steel cannula, 6.5 mm in length, attached to a plastic pedestal (Plastics One, Roanoke, VA) was stereotaxically lowered into one of several brain areas using the following coordinates, with bregma marking zero for the mediolateral (ML) and anteroposterior (AP) directions, and the top of the skull marking zero for the dorsoventral (DV) direction: (1) angular bundle: AP = 7.2 mm, ML = 5.5 mm, DV = −6.5 mm; (2) deep entorhinal cortex (EC): AP = 7.0 mm, ML = 5.8 mm, DV = −6.5 mm; (3) stratum lacunosum moleculare of CA1: AP = 5.9 mm, ML = −5.9 mm, DV = −6.5 mm; (4) molecular layer of the subiculum: AP = −6.25 mm, ML = 5.4 mm, DV = 6.5 mm; (5) the hilus of the dentate gyrus: AP = 5.8 mm, ML = 4.9 mm, DV = −6.5 mm; and (6) lateral ventricle: AP = −0.12 mm, ML = 1.5 mm, DV = −5.5 mm. Only one of these areas in one cerebral hemisphere was targeted in each rat.

The cannula was lowered into the brain till the pedestal touched the skull. The pedestal was then glued to the skull with cyanoacrylate. The cannula and pedestal were connected via plastic tubing to a subcutaneously implanted Alzet osmotic pump (Model 2004, Durect Corp., Cupertino, CA) which delivers a continuous flow of 0.25 μL/h for ~28 days.

Treatment pumps were filled with MSO (2.5 mg/ml; dissolved in Dulbecco's phosphate buffered saline (PBS) to achieve a delivery of 0.625 μg of MSO per hour. Control pumps were filled with PBS. Following placement of the cannula and pedestal, four stainless steel epidural screw electrodes (Plastics One) were implanted to record cortical EEG activity. Two electrodes (one in each hemisphere) were positioned in the epidural space over the dorsal anterior hippocampal formation (AP = −2.0, ML = ±2.5). A third screw electrode was positioned in the epidural space (AP = −8.5, ML = −2.2) to serve as the reference. A fourth electrode, which was positioned in the skull so that it did not contact the brain (AP = −8.5, ML = 1.5), served as the ground. Three additional stainless steel mounting screws (Plastics One) were inserted into the skull to reduce the risk of headcap detachment.

The female socket contacts on the ends of each electrode were inserted into a plastic pedestal (Plastics One), and the entire implant was secured by UV light cured acrylated urethane adhesive (Loctite 3106 Light Cure Adhesive, Henkel Corp., Rocky Hill, CT.) to form a headcap.

Video-intracranial EEG monitoring, seizure quantitation and statistics

The experimental setup for recording video-EEG was adapted from Bertram et al. (1997). The rats were placed individually in custom-made Plexiglas cages. A spring-covered, 6-channel cable was connected to the electrode pedestal on one end and to a commutator (Plastics One) on the other. A second cable connected the commutator to a digital EEG and video recording unit (CEEGraph Vision LTM, Natus/Bio-Logic Systems Corp., San Carlos, CA). Digital cameras with infrared light detection capability were used to record animal behavior (two cages per camera). The digital video signal was encoded and synchronized to the digital EEG signals. Seizures were identified by visual inspection of the EEG record. As detailed in Avoli and Gloor (1994) seizures were defined by EEG characteristics and not just by the duration of the discharge. Specifically, seizures displayed distinct signal changes from background (interictal) activity. Such signal changes included sustained rhythmic or spiking EEG patterns and a clear evolution of signal characteristics from onset to termination. Subclinical seizures were distinguished from clinical seizures by examination of the video record. The start and stop points of seizures were identified by the following commonly used method. By visual inspection of the EEG, we determined a point that was unequivocally within the seizure. Next, we moved backward in time to determine the seizure start time as the first point where the EEG was different from background activity and forward in time to establish the seizure end time. The video record was examined to stage the seizures, using a modification of Racine's criteria (Racine et al., 1973), as follows: Subclinical, no remarkable behavior; stage 1, immobilization, eye blinking, twitching of vibrissae and mouth movements; stage 2, head nodding, often accompanied by facial clonus; stage 3, forelimb clonus; stage 4, rearing; stage 5, rearing, falling and generalized convulsions. Recurrent seizures were defined as a minimum of 2 electrographic seizures that occurred at least 24 h apart.

One way ANOVA was used to test the difference between groups in total number of seizures over 21 days. Repeated measures ANOVA was used to compare the total number of (1) all seizures, (2) nonsevere seizures [stages 1–3], (3) severe seizures [stages 4 and 5], and

(4) the percent of severe seizures out of the total number of seizures over 21 days in 3 day bins (1–3, 4–6, 7–9, 10–12, 13–15, 16–18, 19–21). ANOVAs were followed by a post hoc [Fisher least square difference (LSD) test]. Significance was defined as $p < 0.05$.

Histology

Rats were anesthetized with Isoflurane and perfused transcardially with 0.9% NaCl followed by 4% paraformaldehyde in phosphate buffer (PB; 0.1 M, pH 7.4). The brains were removed and left in the same fixative at 4 °C for 24 h and then transferred to PB. The brains were stored at 4 °C until being sectioned on a Vibratome at 50-μm thickness. Every fifth section was mounted on gelatin-coated slides and stained with cresyl violet. For NeuN staining, the primary antibody used was (MAB377 Millipore Corp., Bellerica, MA.; 1:1000 dilution), and the secondary antibody was biotinylated goat anti-mouse secondary antibody (BA-2000, Vector Laboratories, Burlingame, CA). The Vectastain Elite kit (Vector Laboratories) with 3,3′-diaminobenzidine as the chromogen was used for antibody visualization. The slides were covered and examined under a light microscope. The amount of mechanical damage caused by the injector was quantified by measuring the diameter of the damaged area in cresyl violet stained sections. Mechanical damage for each separate group, as well as for all groups combined, was then correlated with total number of seizures over a 21 day period. The total number of NeuN positive cells in the hilus of the dentate gyrus was also correlated with seizure frequency over 21 days. The hilus was specifically chosen as the area of neuronal quantification based on background literature indicating a positive correlation between neuronal loss in the dentate gyrus with seizure frequency (Groticke et al., 2008; Rattka et al., 2013). Pearson correlation was used for analysis. Significance was defined as $p < 0.05$.

Results

Location of MSO infusion sites

Six brain regions were consistently targeted by microinjections of MSO: the deep EC ($n = 7$, Fig. 1A), the angular bundle ($n = 6$, Fig. 1B), the molecular layer of the subiculum (also referred to as subiculum, $n = 10$, Fig. 1C), the stratum lacunosum-moleculare of CA1 (also referred to as the CA1, $n = 7$, Fig. 1D), the hilus of the dentate gyrus (also referred to as the dentate gyrus, $n = 6$, Fig. 1E), and the lateral ventricle ($n = 6$, not shown). Microinjections into the deep EC (Fig. 1A) fell into layers IV–VI in the lateral subdivision of the structure. Injection locations in the angular bundle (Fig. 1B) fell mainly in the most posterior and medial portion of the structure, spanning the width of the fiber pathway between the deep EC and the pyramidal layer of subiculum. Microinjection locations in the molecular layer of the subiculum (Fig. 1C) and the stratum lacunosum-moleculare of CA1 (Fig. 1D) were directly adjacent to the lateral anterior and lateral posterior portions of the molecular layer of the dentate gyrus, respectively. Microinjection locations in the hilus of the dentate gyrus were not clustered in any particular area; however, some locations were adjacent to the dentate granule cells (Fig. 1E). With respect to the lateral ventricle, most injections occurred above the caudal portion of the nucleus accumbens shell (below and slightly lateral to bregma).

A total of 12 rats were infused with PBS to serve as nonepileptic controls. The injection sites of the PBS treated rats were as follows: deep EC (n = 3), molecular layer of the subiculum (n = 4), stratum lacunosum-moleculare of CA1 (n = 1), and the hilus of the dentate gyrus (n = 4).

Average frequency of seizures over 21 days

We first quantified the number of seizures in the MSO and PBS treated rats by analysis of video-intracranial EEG records continuously collected over a period of 21 days after the onset of intracranial infusion. All of the rats treated with MSO in the Ent–Hip area (Fig. 2), and none of the PBS-infused rats (not shown) developed recurrent seizures. Four of the 6 rats infused with MSO in the lateral ventricle developed recurrent seizures (Fig. 2). The total number of seizures was documented for each rat and averaged for each group. A one-way ANOVA carried out over the average number of seizures over the entire 21-day-period indicated a significant effect of group [$F(5, 36) = 6.43$, $p < 0.001$], suggesting a difference in the total number of seizures based on the site of injection. A post hoc Fisher LSD test indicated that rats receiving MSO into the hilus of the dentate gyrus showed a significantly higher frequency of seizures (1.7 to 12 fold higher) than all other groups ($p < 0.01$). Similarly, rats receiving MSO injections into the CA1 showed a significantly higher frequency of seizures (2.05 to 7.3 fold higher) than all other groups ($p < 0.05$), except the angular bundle and dentate gyrus groups.

EEG patterns after MSO-infusion in different brain regions

We visually inspected all seizures during early (Days 1–3) and late (Days 19–21) epileptogenesis, from two animals in each of the MSO-infused groups. The seizures in the different groups were similar to those described in our previous report (Wang et al., 2009), with the following exceptions. First, some of the seizures in the lateral ventricle group had markedly diminished EEG amplitude, indicating that the seizures may have occurred further away from the recording electrodes compared with the other groups. Second, the seizures in the CA1 and dentate gyrus groups often occurred in clusters, both at early and late time-points. Such clusters were not seen in other groups. The clusters typically occurred over a relatively short duration ranging from 5 min to 1 h. A typical cluster of 3 separate seizures that occurred over ~8 min, 21 days after MSO infusion, is depicted in Fig. 3.

Total number of seizures over 21 days

The effect of MSO infusion site on the daily number of seizures was next evaluated (Fig. 4A). Repeated measures ANOVA over days indicated a significant effect of group [$F(5, 36) = 8.46$, $p < 0.0001$], a significant effect of days [$F(7, 336) = 10.51$, $p < 0.0001$], and a significant group by day interaction [$F(7, 336 = 2.00$, $p = 0.002$], suggesting the presence of a relationship between site of injection and the daily number of seizures experienced over the 21 days of recording. A post hoc Fisher LSD test indicated that during the first 3 days of MSO infusion, rats receiving MSO into the dentate gyrus and the CA1, demonstrated a significantly higher number of seizures than all other groups at all other times with the exception of days 7–9 in the group receiving MSO in the dentate gyrus ($p < 0.0001$, Fig. 4A). The frequency of seizures during days 7–9 in the dentate gyrus group was significantly

higher than all other groups and times, with the exception of days 1–3 in the subiculum, CA1, and dentate gyrus groups (**$p < 0.01$, Fig. 4A). The frequency of seizures during the first three days in the subiculum group was significantly higher than all other time points in that group (* $p < 0.05$, Fig. 4A).

Total number of non-severe (stages 1–3) seizures over 21 days

Analysis of the total number of non-severe seizures indicated a significant effect of group [$F(5, 36) = 9.49$, $p = 0.0001$], a significant effect of day [$F(7, 336) = 18.22$, $p < 0.0001$], and a significant group by day interaction [$F(7, 336) = 2.74$, $p = 0.0001$]. A post hoc Fisher LSD test indicated that non-severe seizures during days 1–3 were significantly higher than all other days in the subiculum ($p < 0.01$), CA1 ($p < 0.0001$), and dentate gyrus groups ($p < 0.0001$). The one exception was days 7–9 in the dentate gyrus group, which was higher than all other days in that group ($p < 0.01$). Rats in the angular bundle group and entorhinal cortex groups did not show a significant alteration in absolute number of non-severe seizures over time (Fig. 4B).

Total number of severe (stages 4–5) seizures over 21 days

The analysis for the total number of severe seizures indicated an effect of group [$F(5, 36) = 4.25$, $p = 0.003$] and an effect of day [$F(7, 336) = 2.34$, $p < 0.05$], with no group by day interaction. A post hoc Fisher LSD test indicated that during the first 3 days, rats infused in the dentate gyrus showed a significantly higher number of stage 4 and 5 seizures than all other groups at all time points, with the exception of days 7–9 in the dentate gyrus group and days 1–3 in the CA1 group ($p < 0.001$, Fig. 4C). Rats in the CA1 group showed a significantly higher number of stage 4 and 5 seizures during the first 3 days than all other groups at all time points, with the exception of rats in the CA1 group at days 10–15 and rats in the dentate gyrus group at days 1–3 and 7–9 ($p < 0.05$, Fig. 4C).

Percent severe seizures out of the total number of seizures over 21 days

We next used repeated measures ANOVA to ask whether the fraction of stage 4 and 5 seizures relative to all types of seizures changes during the 21-day monitoring period. This analysis indicated no effect of group, a significant effect of days [$F(7, 336) = 14.03$, $p < 0.0001$], and no group by days interaction (Fig. 4D). A post hoc Fisher LSD test showed that within the time points for each brain region, rats in the entorhinal cortex group showed a significantly higher fraction of stages 4 and 5 seizures on days 10–21 compared to days 1–6 [($p < 0.05$) when comparing days 10–15 to days 1–6; $p < 0.0001$ when comparing days 16–21 to days 1–6, Fig. 4D)]. Rats in the angular bundle and subiculum groups showed a significantly higher fraction of stages 4–5 seizures during days 13–21 compared to days 1–6 ($p < 0.01$, Fig. 4D). Rats in the CA1 group showed a significantly higher fraction of stages 4–5 seizures during days 13–16 when compared to days 1–3 ($p < 0.01$, Fig. 4D). Finally, rats in the dentate gyrus group showed a significantly higher fraction of severe seizures during days 19–21 when compared to days 1–6 (* $p < 0.05$).

Neuropathology

Lastly, we correlated the extent of mechanical damage of the infusion site and the neuronal density in the hilus of the dentate gyrus with the total number of seizures over 21 days. All rats showed mechanical damage around the injection site as indicated in Fig. 1. The diameter of mechanical damage in each MSO-infused group, as well as in all groups combined, did not correlate with average seizure frequency over 21 days. Quantification of neuronal loss in the dentate gyrus with NeuN staining for rats in all groups combined, indicated that the number of neurons present in the hilus of the dentate gyrus correlated negatively with the total number of seizures over 21 days ($R = -0.573$; $p < 0.005$) (Fig. 5).

Discussion

We have demonstrated the effects of GS inhibition in specific brain areas on the temporal evolution of seizures (i.e. epileptogenesis) through site-specific infusions of MSO. All animals infused with MSO into the Ent–Hip area exhibited recurrent, frequent seizures during the first 3 days of infusion and persistent but less frequent seizures for the remaining 3 week recording period. In contrast, only a fraction of animals infused with MSO into the lateral ventricle had recurrent seizures, which occurred at a lower frequency compared with the other MSO infused groups. Infusion of MSO into the hilus of the dentate gyrus resulted in the highest total number of seizures over the entire recording period. Infusion of MSO into the hilus of the dentate gyrus, the stratum lacunosum-moleculare of the CA1, and the molecular layer of the subiculum resulted in a high frequency of seizures during the first 3 days of infusion with a dramatic decrease in seizure frequency for the rest of the recording period. Infusion of MSO into all brain regions studied, with the exception of the lateral ventricle, led to a change in the composition of seizure severity over time. Low-grade (stages 1–3) seizures were more prevalent early during MSO infusion, while severe (stages 4–5) seizures were more prevalent later.

We observed that MSO infusion into the Ent–Hip area more effectively resulted in chronic seizures than infusion of equivalent doses into the lateral ventricle. This finding may be explained by one of several mechanisms. Infusion of MSO directly into the tissue rather than by the intracerebroventricular (ICV) route is likely to restrict diffusion of MSO and lead to higher tissue concentrations, with persistently increased target effects of the drug. Furthermore, ICV infusion is likely to affect a wider brain distribution than intraparenchymal administration, resulting in more diffuse central nervous system (CNS) effects. For example, ICV infusion resulted in a high fraction of hindlimb clonus convulsions (approximately 67% observed during the first week). This type of seizure is rarely seen in the other treatment groups, suggesting that ICV infusion rapidly affects areas beyond the limbic system, such as the motor cortex.

We further demonstrated that infusion of MSO into the dentate gyrus, CA1 or subiculum resulted in a high initial frequency of seizures, suggesting that the microanatomical infusion target is a critical determinant for how seizures initially manifest and evolve over time. While the heterogeneity in seizure patterns may in part be attributed to differences in diffusion of MSO in various brain regions, e.g. increased diffusion in the ventricular system and along fiber bundles vs. when given in gray matter areas, the heterogeneity may also be

explained by regional differences in neuronal properties, as discussed in detail below. Seizures were also found to occur in clusters in the CA1 and dentate gyrus areas, suggesting both the presence of a relatively longer duration of vulnerability in these animals during which time multiple seizures are initiated and expressed and their suitability as a model for the generation of clusters of seizures in human epilepsy. The reason for the low threshold for seizure initiation during this time-period in the CA1 and dentate gyrus areas remains to be determined.

Despite a continuous infusion of MSO into all the brain regions studied, we observed a dramatic reduction in seizure frequency starting on day 1 in the CA1 and dentate gyrus infused groups and on days 2 or 3 in the other groups. While the mechanism of the seizure decline is poorly understood, several explanations are plausible. The decrease in seizure frequency might be due to increased GABA-mediated inhibition. The GABAergic system is exquisitely sensitive to seizure-induced plastic changes involving synaptic connections, neurotransmitter receptors, ion channels, GABA uptake and GABA metabolism (Kaila et al., 2014). Many of these changes are thought to promote seizures, such as loss of hippocampal interneurons with decreased GABAergic inhibition (Sloviter, 1987), and decreased expression of $GABA_A$ receptors (Naylor et al., 2005) and the neuronal K–Cl cotransporter (KCC2) (Lee et al., 2010). However, some changes are thought to facilitate inhibition, such as an increase in spontaneous inhibitory postsynaptic currents after memantine-induced seizures (He and Bausch, 2014), an increase in extracellular GABA levels after pilocarpine-induced seizures (Meurs et al., 2008), and mossy fiber sprouting with increased excitatory input onto surviving hilar GABAergic neurons. It is interesting to note that rats with the most pronounced loss of hilar neurons had the highest frequency of seizures, suggesting that surviving hilar neurons indeed are important for reducing seizure activity.

Because astrogliosis is a common and rapid reaction to seizures, it is possible that an increased number of astrocytes along with compensatory upregulation of GS may overcome part of the inhibition caused by MSO, thus explaining the initial seizure decline. The MSO infusion pump has been manufactured and tested to consistently deliver a continuous infusion of 0.25 μL/h for 4 weeks with an infusion rate variability (coefficient of variation) of less than 10%; thus the dramatic decline in seizure activity at days 2–3 cannot be explained by decreased delivery of MSO to the tissue.

Infusion of MSO into all brain regions studied, with the exception of the lateral ventricle, resulted in an increase in the ratio of high-grade (stages 4–5) to low-grade (stages 1–3) seizures over time. We observed the most significant increase when MSO was infused in the entorhinal cortex, and a somewhat less significant increase when infused into the hippocampus proper. It may be argued that the change in seizure severity is driven by the dramatic reduction in seizure frequency, particularly in low-grade seizures, during the first few days of MSO infusion. However, because the change in seizure severity also continues to evolve at later stages of MSO infusion, a process of cellular, metabolic and electrophysiological plasticity that operates over the entire 21-day monitoring period is likely to be involved. The nature and temporal evolution of these changes are unknown, particularly in relationship to the loss of GS. Further studies are clearly needed to address these issues.

The observation that the temporal progression of seizure severity is highly significant after infusion of MSO into the entorhinal cortex emphasizes that this region, along with the hippocampus proper, is important in the pathophysiology of MTLE. The entorhinal cortex represents one of the main sources of efferent fibers to the hippocampal formation. Neurons in layer II of the entorhinal cortex project to the dentate granule cells as the perforant path (Lomo, 1971), and neurons in layer III of the entorhinal cortex projects to pyramidal cells in the CA1 as the temporo-ammonic path (Barbarosie et al., 2000). Moreover, the hippocampal formation feeds back to the entorhinal cortex via projections from the CA1 and subiculum to the deep layers (V–VI) of the structure (Jones and Woodhall, 2005). The involvement of the entorhinal cortex in MTLE is suggested by several observations. First, depth electrode recordings in patients with MTLE have shown that ictal EEG activity often involves both the entorhinal cortex and the hippocampal formation. The seizures sometimes start in the entorhinal cortex before they spread to the hippocampal formation (Spencer and Spencer, 1994). Studies have further demonstrated that an incomplete removal of the entorhinal cortex results in a less successful outcome of surgery (Siegel et al., 1990). Animal studies have also shown that “hippocampal” seizures often originate in the entorhinal cortex (Jensen and Yaari, 1988; Swartzwelder et al., 1987; Walther et al., 1986). Furthermore, neurons are preferentially lost in layer III of the entorhinal cortex in patients with MTLE and in relevant animal models of the disorder (Du et al., 1995, 1993; Gastaut et al., 1959). In addition, activated microglial cells and reactive astrocytosis are frequently present in the entorhinal cortex in the chronic phase of the pilocarpine and kainic acid models of MTLE. It has been proposed that the glial changes may contribute to increased excitability of the entorhinal–hippocampal region (Alvestad et al., 2007; Cohen et al., 2002; Drexel et al., 2012; Jung et al., 2009) by increasing extracellular glutamate levels (Angulo et al., 2004).

In this study we demonstrated that seizures are most frequent in the first few days after implantation of the MSO pump, with the highest seizure frequency observed when MSO is infused into the CA1 and dentate gyrus and lowest when infused into the entorhinal cortex and angular bundle. One may postulate that if kindling is occurring in our model, the group with the highest initial frequency of seizures would show over time a higher frequency of seizures (both non-severe and severe) than the group with a lower initial frequency of seizures. On the contrary, we observed that the frequency of seizures during the later time period was independent of the initial frequency of seizures. Furthermore, rats with the lowest initial frequency of seizures progressed most quickly to severe seizures and rats with the initial highest frequency of seizures progressed most slowly to severe seizures. This lack of a kindling effect is an interesting characteristic of the MSO model that warrants further study.

We have previously shown that the paradigm of MSO infusion used here inhibits brain GS in vivo (Eid et al., 2008). However, it is important to note that MSO also has other biological effects, which could contribute to the findings observed here. For example, MSO has been shown to increase glycogen content in astrocytes (Delorme and Hevor, 1985) and decrease levels of glutathione in the brain (Shaw and Bains, 2002). MSO can also cause neuronal excitation by mechanisms other than GS inhibition (Kam and Nicoll, 2007). While we have not detected a reduction in brain glutathione concentrations in our model (Eid et al., 2008), the other effects could possibly contribute to the present findings. A more specific

approach to study GS inhibition would be to use GS knockout mice. However, systemic or astrocyte-specific GS knockouts are lethal in utero and shortly after birth (He et al., 2010, 2007). Brain site-specific knockouts of the gene, which are not yet available, will therefore be necessary to validate our findings.

Previous studies have stimulated, either electrically or chemically, different areas of the Ent–Hip network to induce seizures including the CA1 (Gilbert et al., 2000), CA3 (Bragin et al., 2005) dentate gyrus (Zhang et al., 2001), angular bundle (Sardo et al., 2008), and entorhinal cortex (Heidarianpour et al., 2006). However, to our knowledge this is the first investigation that pharmacologically manipulated GS in several locations within the Ent–Hip network in the same study, thus allowing for direct comparisons of the site-specific effects of MSO treatment on the frequency, severity, and the temporal progression of seizures. Our results will likely lead to a better understanding of how different regions within the Ent–Hip area may modulate seizures and epileptogenesis. We propose that the intracerebral MSO model is well suited to answer specific questions pertinent to epileptic networks, epileptogenesis, and treatment of MTLE. Finally, our work supports the hypothesis that GS is critically involved in the pathophysiology of MTLE and that the anatomical site of GS inhibition determines the pattern and temporal evolution of recurrent seizures in the MSO model of MTLE.

Supplementary Material

Refer to Web version on PubMed Central for supplementary material.

Acknowledgements

The authors would like to thank Ms. Ilona Kovacs for excellent technical assistance. TE, HZ and RD are supported by grants from the National Institutes of Health (NIH): NINDS K08 NS058674 and R01 NS070824. This work was also made possible by CTSA Grant number UL1 TR000142 from the National Center for Advancing Translational Science (NCATS), a component of the National Institutes of Health (NIH). Its contents are solely the responsibility of the authors and do not necessarily represent the official view of NIH.

References

Alvestad S, Goa PE, Qu H, Risa O, Brekken C, Sonnewald U, Haraldseth O, Hammer J, Ottersen OP, Haberg A. In vivo mapping of temporospatial changes in manganese enhancement in rat brain during epileptogenesis. NeuroImage. 2007; 38:57–66. [PubMed: 17822925]

Angulo MC, Kozlov AS, Charpak S, Audinat E. Glutamate released from glial cells synchronizes neuronal activity in the hippocampus. J. Neurosci. 2004; 24:6920–6927. [PubMed: 15295027]

Avoli, M.; Gloor, P. Pathophysiology of focal and generalized convulsive seizures versus that of generalized non-convulsive seizures.. In: Wolf, P., editor. Epileptic Seizures and Syndromes. John Libby Eurotext Ltd.; Montrouge, France: 1994. p. 547-561.

Barbarosie M, Louvel J, Kurcewicz I, Avoli M. CA3-released entorhinal seizures disclose dentate gyrus epileptogenicity and unmask a temporoammonic pathway. J. Neurophysiol. 2000; 83:1115–1124. [PubMed: 10712442]

Bertram EH, Williamson JM, Cornett JF, Chen ZF. Design and construction of a long-term continuous video-EEG monitoring unit for simultaneous recording of multiple small animals. Brain Res. Brain Res. Protoc. 1997; 1997:85–97. [PubMed: 9438076]

Bragin A, Azizyan A, Almajano J, Wilson CL, Engel J Jr. Analysis of chronic seizure onsets after intrahippocampal kainic acid injection in freely moving rats. Epilepsia. 2005; 46:1592–1598. [PubMed: 16190929]

Bruneau EG, McCullumsmith RE, Haroutunian V, Davis KL, Meador-Woodruff JH. Increased expression of glutaminase and glutamine synthetase mRNA in the thalamus in schizophrenia. Schizophr. Res. 2005; 75:27–34. [PubMed: 15820321]

Cohen I, Navarro V, Clemenceau S, Baulac M, Miles R. On the origin of interictal activity in human temporal lobe epilepsy in vitro. Science. 2002; 298:1418–1421. [PubMed: 12434059]

Danbolt NC. Glutamate uptake. Prog. Neurobiol. 2001; 65:1–105. [PubMed: 11369436]

de Guzman P, Inaba Y, Biagini G, Baldelli E, Mollinari C, Merlo D, Avoli M. Subiculum network excitability is increased in a rodent model of temporal lobe epilepsy. Hippocampus. 2006; 16:843–860. [PubMed: 16897722]

Delorme P, Hevor TK. Glycogen particles in methionine sulfoximine epileptogenic rodent brain and liver after the administration of methionine and actinomycin D. Neuropathol. Appl. Neurobiol. 1985; 11:117–128. [PubMed: 4022258]

Drexel M, Preidt AP, Sperk G. Sequel of spontaneous seizures after kainic acid-induced status epilepticus and associated neuropathological changes in the subiculum and entorhinal cortex. Neuropharmacology. 2012; 63:806–817. [PubMed: 22722023]

Du F, Eid T, Lothman EW, Kohler C, Schwarcz R. Preferential neuronal loss in layer III of the medial entorhinal cortex in rat models of temporal lobe epilepsy. J. Neurosci. 1995; 15:6301–6313. [PubMed: 7472396]

Du F, Whetsell WO Jr. Abou-Khalil B, Blumenkopf B, Lothman EW, Schwarcz R. Preferential neuronal loss in layer III of the entorhinal cortex in patients with temporal lobe epilepsy. Epilepsy Res. 1993; 16:223–233. [PubMed: 8119273]

During MJ, Spencer DD. Extracellular hippocampal glutamate and spontaneous seizure in the conscious human brain. Lancet. 1993; 341:1607–1610. [PubMed: 8099987]

Eid T, Ghosh A, Wang Y, Beckstrom H, Zaveri HP, Lee TS, Lai JC, Malthankar-Phatak GH, de Lanerolle NC. Recurrent seizures and brain pathology after inhibition of glutamine synthetase in the hippocampus in rats. Brain. 2008; 131:2061–2070. [PubMed: 18669513]

Eid T, Thomas MJ, Spencer DD, Runden-Pran E, Lai JC, Malthankar GV, Kim JH, Danbolt NC, Ottersen OP, de Lanerolle NC. Loss of glutamine synthetase in the human epileptogenic hippocampus: possible mechanism for raised extracellular glutamate in mesial temporal lobe epilepsy. Lancet. 2004; 363:28–37. [PubMed: 14723991]

Gastaut H, Toga M, Roger J, Gibson WC. A correlation of clinical, electroencephalographic and anatomical findings in nine autopsied cases of “temporal lobe epilepsy”. Epilepsia. 1959; 1:56–85.

Gilbert TH, Hannesson DK, Corcoran ME. Hippocampal kindled seizures impair spatial cognition in the Morris water maze. Epilepsy Res. 2000; 38:115–125. [PubMed: 10642039]

Groticke I, Hoffmann K, Loscher W. Behavioral alterations in a mouse model of temporal lobe epilepsy induced by intrahippocampal injection of kainate. Exp. Neurol. 2008; 213:71–83. [PubMed: 18585709]

He S, Bausch SB. Synaptic plasticity in glutamatergic and GABAergic neurotransmission following chronic memantine treatment in an in vitro model of limbic epileptogenesis. Neuropharmacology. 2014; 77:379–386. [PubMed: 24184417]

He Y, Hakvoort TB, Vermeulen JL, Labruyere WT, De Waart DR, Van Der Hel WS, Ruijter JM, Uylings HB, Lamers WH. Glutamine synthetase deficiency in murine astrocytes results in neonatal death. Glia. 2010; 58:741–754. [PubMed: 20140959]

He Y, Hakvoort TB, Vermeulen JL, Lamers WH, Van Roon MA. Glutamine synthetase is essential in early mouse embryogenesis. Dev. Dyn. 2007; 236:1865–1875. [PubMed: 17557305]

Heidarianpour A, Sadeghian E, Mirnajafi-Zadeh J, Fathollahi Y, Mohammad-Zadeh M. Anticonvulsant effects of N6-cyclohexyladenosine microinjected into the CA1 region of the hippocampus on entorhinal cortex-kindled seizures in rats. Epileptic Disord. 2006; 8:259–266. [PubMed: 17150438]

Jensen MS, Yaari Y. The relationship between interictal and ictal paroxysms in an in vitro model of focal hippocampal epilepsy. Ann. Neurol. 1988; 24:591–598. [PubMed: 2849367]

Jones RS, Woodhall GL. Background synaptic activity in rat entorhinal cortical neurones: differential control of transmitter release by presynaptic receptors. J. Physiol. 2005; 562:107–120. [PubMed: 15498804]

Jung KH, Chu K, Lee ST, Kim JH, Kang KM, Song EC, Kim SJ, Park HK, Kim M, Lee SK, Roh JK. Region-specific plasticity in the epileptic rat brain: a hippocampal and extrahippocampal analysis. Epilepsia. 2009; 50:537–549. [PubMed: 19054393]

Kaila K, Ruusuvuori E, Seja P, Voipio J, Puskarjov M. GABA actions and ionic plasticity in epilepsy. Curr. Opin. Neurobiol. 2014; 26:34–41. [PubMed: 24650502]

Kam K, Nicoll R. Excitatory synaptic transmission persists independently of the glutamate-glutamine cycle. J. Neurosci. 2007; 27:9192–9200. [PubMed: 17715355]

Lee HH, Jurd R, Moss SJ. Tyrosine phosphorylation regulates the membrane trafficking of the potassium chloride co-transporter KCC2. Mol. Cell. Neurosci. 2010; 45:173–179. [PubMed: 20600929]

Lee Y, Son H, Kim G, Kim S, Lee DH, Roh GS, Kang SS, Cho GJ, Choi WS, Kim HJ. Glutamine deficiency in the prefrontal cortex increases depressive-like behaviours in male mice. J. Psychiatry Neurosci. 2013; 38:183–191. [PubMed: 23031251]

Lomo T. Patterns of activation in a monosynaptic cortical pathway: the perforant path input to the dentate area of the hippocampal formation. Exp. Brain Res. 1971; 12:18–45. [PubMed: 5543199]

Martinez-Hernandez A, Bell KP, Norenberg MD. Glutamine synthetase: glial localization in brain. Science. 1977; 195:1356–1358. [PubMed: 14400]

Meurs A, Clinckers R, Ebinger G, Michotte Y, Smolders I. Seizure activity and changes in hippocampal extracellular glutamate, GABA, dopamine and serotonin. Epilepsy Res. 2008; 78:50–59. [PubMed: 18054462]

Naylor DE, Liu H, Wasterlain CG. Trafficking of GABA(A) receptors, loss of inhibition, and a mechanism for pharmacoresistance in status epilepticus. J. Neurosci. 2005; 25:7724–7733. [PubMed: 16120773]

Olney, JW. Neurotoxicity of excitatory amino acids.. In: McGeer, EG.; Olney, JW.; McGeer, PL., editors. Kainic Acid as a Tool in Neurobiology. Raven Press; New York, NY: 1978. p. 37-70.

Olney JW, Sharpe LG, Feigin RD. Glutamate-induced brain damage in infant primates. J. Neuropathol. Exp. Neurol. 1972; 31:464–488. [PubMed: 4626680]

Perez EL, Lauritzen F, Wang Y, Lee TS, Kang D, Zaveri HP, Chaudhry FA, Ottersen OP, Bergersen LH, Eid T. Evidence for astrocytes as a potential source of the glutamate excess in temporal lobe epilepsy. Neurobiol. Dis. 2012; 47:331–337. [PubMed: 22659305]

Pitkanen A, Tuunanen J, Halonen T. Subiculum presubiculum and parasubiculum have different sensitivities to seizure-induced neuronal damage in the rat. Neurosci. Lett. 1995; 192:65–68.

Racine RJ, Burnham WM, Gartner JG, Levitan D. Rates of motor seizure development in rats subjected to electrical brain stimulation: strain and inter-stimulation interval effects. Electroencephalogr. Clin. Neurophysiol. 1973; 35:553–556. [PubMed: 4126463]

Rajkowska G, Stockmeier CA. Astrocyte pathology in major depressive disorder: insights from human postmortem brain tissue. Curr. Drug Targets. 2013; 14:1225–1236. [PubMed: 23469922]

Rattka M, Brandt C, Loscher W. The intrahippocampal kainate model of temporal lobe epilepsy revisited: epileptogenesis, behavioral and cognitive alterations, pharmacological response, and hippoccampal damage in epileptic rats. Epilepsy Res. 2013; 103:135–152. [PubMed: 23196211]

Robinson SR. Changes in the cellular distribution of glutamine synthetase in Alzheimer's disease. J. Neurosci. Res. 2001; 66:972–980. [PubMed: 11746426]

Rosati A, Marconi S, Pollo B, Tomassini A, Lovato L, Maderna E, Maier K, Schwartz A, Rizzuto N, Padovani A, Bonetti B. Epilepsy in glioblastoma multiforme: correlation with glutamine synthetase levels. J. Neurooncol. 2009; 93:319–324. [PubMed: 19183851]

Sardo P, D'Agostino S, Carletti F, Rizzo V, La Grutta V, Ferraro G. Lamotrigine differently modulates 7-nitroindazole and l-arginine influence on rat maximal dentate gyrus activation. J. Neural Transm. 2008; 115:27–34. [PubMed: 17994188]

Shaw CA, Bains JS. Synergistic versus antagonistic actions of glutamate and glutathione: the role of excitotoxicity and oxidative stress in neuronal disease. Cell. Mol. Biol. (Noisy-le-grand). 2002; 48:127–136. [PubMed: 11990449]

Siegel AM, Wieser HG, Wichmann W, Yasargil GM. Relationships between MR-imaged total amount of tissue removed, resection scores of specific mediobasal limbic subcompartments and clinical

outcome following selective amygdalohippocampectomy. Epilepsy Res. 1990; 6:56–65. [PubMed: 2357956]

Sloviter RS. Decreased hippocampal inhibition and a selective loss of interneurons in experimental epilepsy. Science. 1987; 235:73–76. [PubMed: 2879352]

Spencer SS, Spencer DD. Entorhinal–hippocampal interactions in medial temporal lobe epilepsy. Epilepsia. 1994; 35:721–727. [PubMed: 8082614]

Steffens M, Huppertz HJ, Zentner J, Chauzit E, Feuerstein TJ. Unchanged glutamine synthetase activity and increased NMDA receptor density in epileptic human neocortex: implications for the pathophysiology of epilepsy. Neurochem. Int. 2005; 47:379–384. [PubMed: 16095760]

Swartzwelder HS, Lewis DV, Anderson WW, Wilson WA. Seizure-like events in brain slices: suppression by interictal activity. Brain Res. 1987; 410:362–366. [PubMed: 3594246]

Toyoda I, Bower MR, Leyva F, Buckmaster PS. Early activation of ventral hippocampus and subiculum during spontaneous seizures in a rat model of temporal lobe epilepsy. J. Neurosci. 2013; 33:11100–11115. [PubMed: 23825415]

van der Hel WS, Notenboom RG, Bos IW, van Rijen PC, van Veelen CW, de Graan PN. Reduced glutamine synthetase in hippocampal areas with neuron loss in temporal lobe epilepsy. Neurology. 2005; 64:326–333. [PubMed: 15668432]

Walther H, Lambert JD, Jones RS, Heinemann U, Hamon B. Epileptiform activity in combined slices of the hippocampus, subiculum and entorhinal cortex during perfusion with low magnesium medium. Neurosci. Lett. 1986; 69:156–161. [PubMed: 3763042]

Wang Y, Zaveri HP, Lee TS, Eid T. The development of recurrent seizures after continuous intrahippocampal infusion of methionine sulfoximine in rats: a video-intracranial electroencephalographic study. Exp. Neurol. 2009; 220:293–302. [PubMed: 19747915]

Zhang XR, Han D, Tang YF, Liu ML, Yin SJ. Possible role of dentate gyrus in greneration of rat temporal lobe epilepsy induced by electrical stimulation. Sheng li xue bao. 2001; 53:235–239. [PubMed: 12589411]

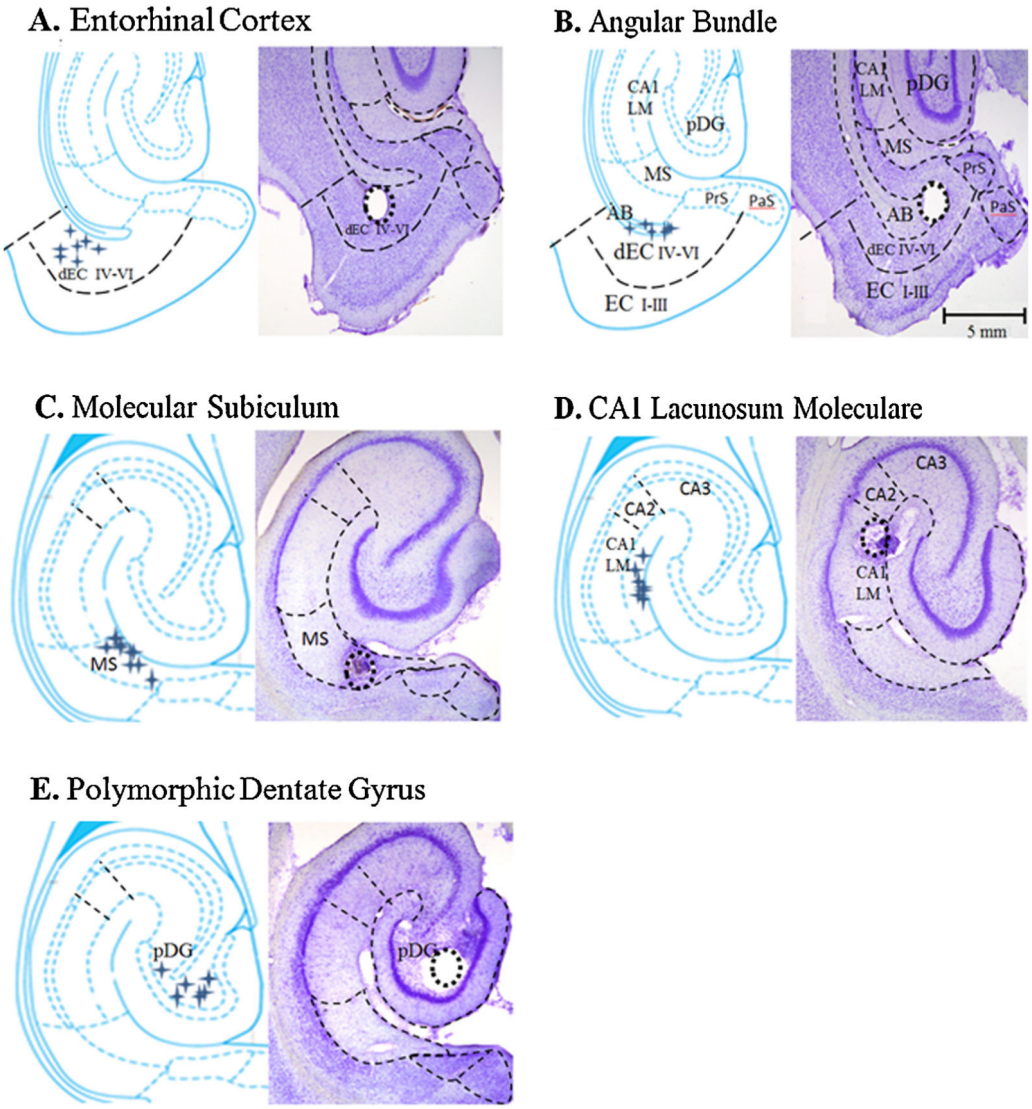

Figure 1.

MSO infusion sites in the rat entorhinal–hippocampal (Ent–Hip) area. The line drawings illustrate the main anatomical subdivisions of the Ent–Hip area with all injection sites represented by crosshairs. Next to each line drawing is a representative Nissl-stained section depicting the injection site. The sites targeted are (A) layers IV–VI of the deep entorhinal cortex [dEC IV–VI] (*n* = 7); (B) the angular bundle [AB] (*n* = 6); (C) the molecular layer of the subiculum [MS] (*n* = 10; (D) the stratum lacunosum moleculare of area CA1 [CA1 LM] (*n* = 7); (*n* = 10); and (E) [the hilus of the dentate gyrus [hDG] (*n* = 6)]. Abbreviations: PaS, parasubiculum; PrS, presubiculum. Thick dashed lines refer to the borders between the main subfields of the region. Scale bar = 5 mm.

Rat #	Brain Region	1	2	3	4	5	6	7	8	9	10	11	12	13	14	15	16	17	18	19	20	21	Total Seizures	Average
11	Lateral Ventricle	0	0	0	0	0	0	0	0	0	0	0	0	0	0	0	0	0	0	0	0	0	0	3.6 ± 2.2
12	Lateral Ventricle	0	11	0	0	0	0	0	0	0	0	0	0	0	0	0	0	0	0	0	0	0	11	
13	Lateral Ventricle	0	0	0	1		1	0	0	1	1	5	1	0	1								11	
14	Lateral Ventricle	0	0	0	0	1	0	2	0	2	0	0	3	0	0	0	0	3	0	0	2	0	13	
15	Lateral Ventricle	5	0	0	2	0	0	0	0	0	0	0	0	0	0	0	0	0	0	0	0	0	7	
16	Lateral Ventricle	0	3	12	0	1	0	0	0	0	0	0	0	0	0	0	0	0	0	0	0	0	16	
35	Deep Entorhinal Cortex	3	5	0	0	1	0	2	2	1	2	2	0	4	1	1	2	2	1	2	1	1	33	25.8 ± 2.8
36	Deep Entorhinal Cortex	3	4	2	1	1	0	3	0	1	0	1	0	3	0	0	0	1	0	2	0	1	23	
37	Deep Entorhinal Cortex	4	3	0	0	1	1	1	2	1	1	1	1	0	1	1	2	1	1	1	1	1	25	
38	Deep Entorhinal Cortex	6	5	2	0	1	2	0	3	1	0	1	0	0	0	0	0	0	0	0	0	0	21	
13	Deep Entorhinal Cortex	0	0	0	0	2	2	2	2	1	2	0	3	2	1	2	2	1	1	3	1	1	28	
15	Deep Entorhinal Cortex	5	1	0	0	1	0	2	3	2	1	5	1	0	0	1	1	2	0	1	1	1	28	
18	Deep Entorhinal Cortex	0	0	0	0	0	0	0	0	0	0	0	0	0	0	0	0	0	1	4	6	0	11	
20	Angular Bundle	2	12	0	1	3	2	1	1	0	0	1	0	1		0	1	1	1	0	1	0	28	35.5 ± 4.5
24	Angular Bundle	11	18	0	0	6	4	1	2	2	1	1	1	1	0	1	1	0	1	0	1	1	53	
26	Angular Bundle	1	0	0	0	0	4	5	2	2	3	1	1	1	0	1	2	2	0	2	3	1	31	
30	Angular Bundle	6	4	1	0	0	5	1	0	1	0	1	0	0	0	0	1	0	0	2	0	1	23	
34	Angular Bundle	5	6	0	2	1	2	3	2	2	0	1	1	1	1	2	0	1	0	2	0	2	34	
24	Angular Bundle	0	2	1	1	3	0	3	10	17	5	0	0	0	0	0	1	0	0	1	0	0	44	
2	Molecular Subiculum	25	8	3	0	0	0	0	0	0	0	0	0	2	0	0	0	0	1	3	0	0	42	33.9 ± 2.6
3	Molecular Subiculum	11	7	0	0	2	0	5	4	3	0	2	8	0	0	0	0	1	2	0	0	0	45	
4	Molecular Subiculum	8	12	1	0	0	6	2	0	0	0	2	1	1	0	1	1	1	2	0	1	2	41	
11	Molecular Subiculum	9	0	0	1	1	1	1	0	1	1	3	0	0	0	1	3	1	0	0	0	2	25	
12	Molecular Subiculum	4	6	2	3	0	0	1	2	0	0	1	1	1	0	1	0	0	1	0	1	3	27	
21	Molecular Subiculum	15	14	0	0	0	0	2	1	0	1	0	0	1	1	1	1	0	0	1	1	0	39	
23	Molecular Subiculum	7	25	0	0	0	2	0	0	2	2	1	0	0	1	1	1	2	0	1	1	0	46	
39	Molecular Subiculum	4	4	0	0	2	2	3	0	4	0	2	1	1	0	2	0	0	0	1	0	2	28	
25	Molecular Subiculum	1	7	0	2	3	1	1	1	0	1	0	2	0	0	1	0	1	1	0	0	0	22	
26	Molecular Subiculum	11	7	0	0	2	2	3	0	0	2	1	1	0	0	0	0	0	0	0	0	0	29	
1	CA1 Lacunosum Moleculare	28	7	0	0	0	0	2	3	0	0	0	0	0	0	0	0	0	0	0	0	0	40	70.1 ± 15.3 *
5	CA1 Lacunosum Moleculare	32	36	17	0	0	0	0	1	2	2	1	0	0	6	5	4	2	3	5	0	0	116	
27	CA1 Lacunosum Moleculare	46	15	6	4	0	0	0	0	0	3	3	1	0	0	1	2	1	2	0	0	0	84	
31	CA1 Lacunosum Moleculare	51	39	5	0	0	0	0	1	0	6	0	1	1	3	5	1	0	0	12	1	0	126	
33	CA1 Lacunosum Moleculare	14	1	0	0	0	1	2	0	0	0	1	2	1	1	1	1	1	0	0	1	1	28	
29	CA1 Lacunosum Moleculare	19	5	0	0	0	0	0	0	0	0	0	0	0	0	0	0	0	0	0	0	0	24	
31	CA1 Lacunosum Moleculare	0	13	5	0	0	0	1	1	2	0	0	1	1	0	4	3	0	1	0	0	1	33	
3	Polymorphic DG	0	0	0	4	18	36	63	45	82	41	4	0	0	0	0	0	0	0	0	0	0	293	118 ± 33.7 **
7	Polymorphic DG	18	6	0	0	0	0	0	0	0	0	3	0	0	0	0	3	0	0	1	13	0	44	
8	Polymorphic DG	38	11	0	0	0	1	1	0	2	1	1	0	0	0	22	1	0	0	1	1	2	82	
1	Polymorphic DG	21	22	1	1	0	0	0	0	2	2	1	1	2	3	2	2	2	0	4	1	2	69	
6	Polymorphic DG	33	1	0	0	0	0	0	2	4	0	0	0	2	1	2	3	0	1	2	11	13	75	
12	Polymorphic DG	74	75	34	0	1	0	1	0	0	0	0	0	0	0	0	0	0	0	0	0	0	185	

Figure 2.

Daily (columns 1–21), total (second to last column) and average (last column) frequency of electrographic seizures in all of the MSO infused rats during the 21-day monitoring period. Colors are used to highlight seizure frequencies as follows: yellow, 1–14 seizures/day; blue, 15–30 seizures/day; red, 31–50 seizures/day; black ≥51 seizures/day. Note the presence of very frequent seizures during the first 2 days in rats injected into either the stratum lacunosum-moleculare of the CA1 or the hilus of the dentate gyrus. Abbreviations: DG, dentate gyrus; CA1, hippocampal subfield Cornu Ammonis 1. ** $p < 0.01$, * $p < 0.05$ when compared to all other groups with the exception of CA1 and dentate gyrus. All values are provided as mean ± SEM. (For interpretation of the references to color in this figure legend, the reader is referred to the web version of this article.)

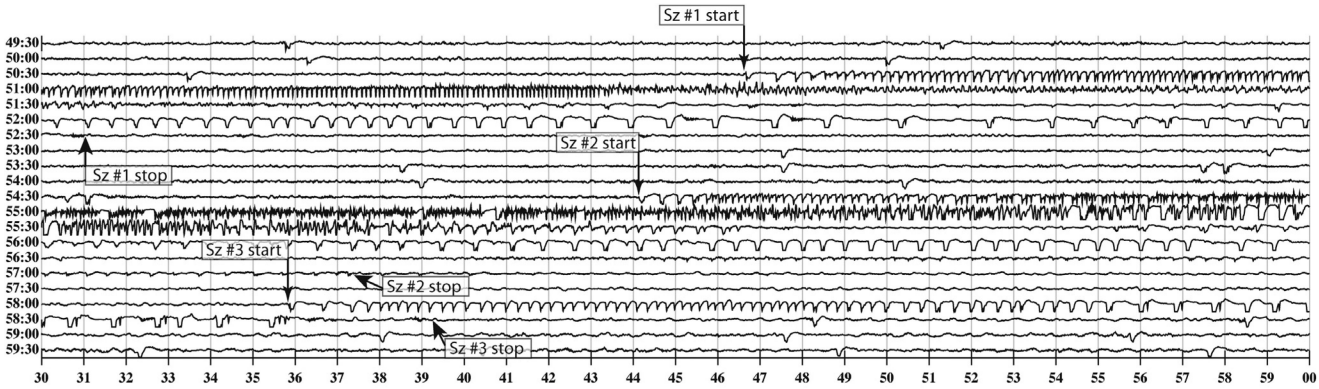

Figure 3.

Six hundred and thirty seconds of continuous icEEG recorded from a screw electrode placed over the right temporal lobe in an animal infused with MSO in the hilus of the dentate gyrus. The data were recorded at the late time-point of epileptogenesis, on Day 21 from 03:49:30 to 04:00:00 AM. Three seizures (indicated with arrows) were expressed over approximately 8 min during this short recording: (1) between 03:50:46 and 03:52:30 AM (Racine stage 3), (2) between 03:54:44 and 03:56:30 AM (Racine stage 1), and (3) between 03:58:05 and 03:58:39 AM (Subclinical seizure). These seizures are similar to those described by us in a prior study (Wang et al., 2009).

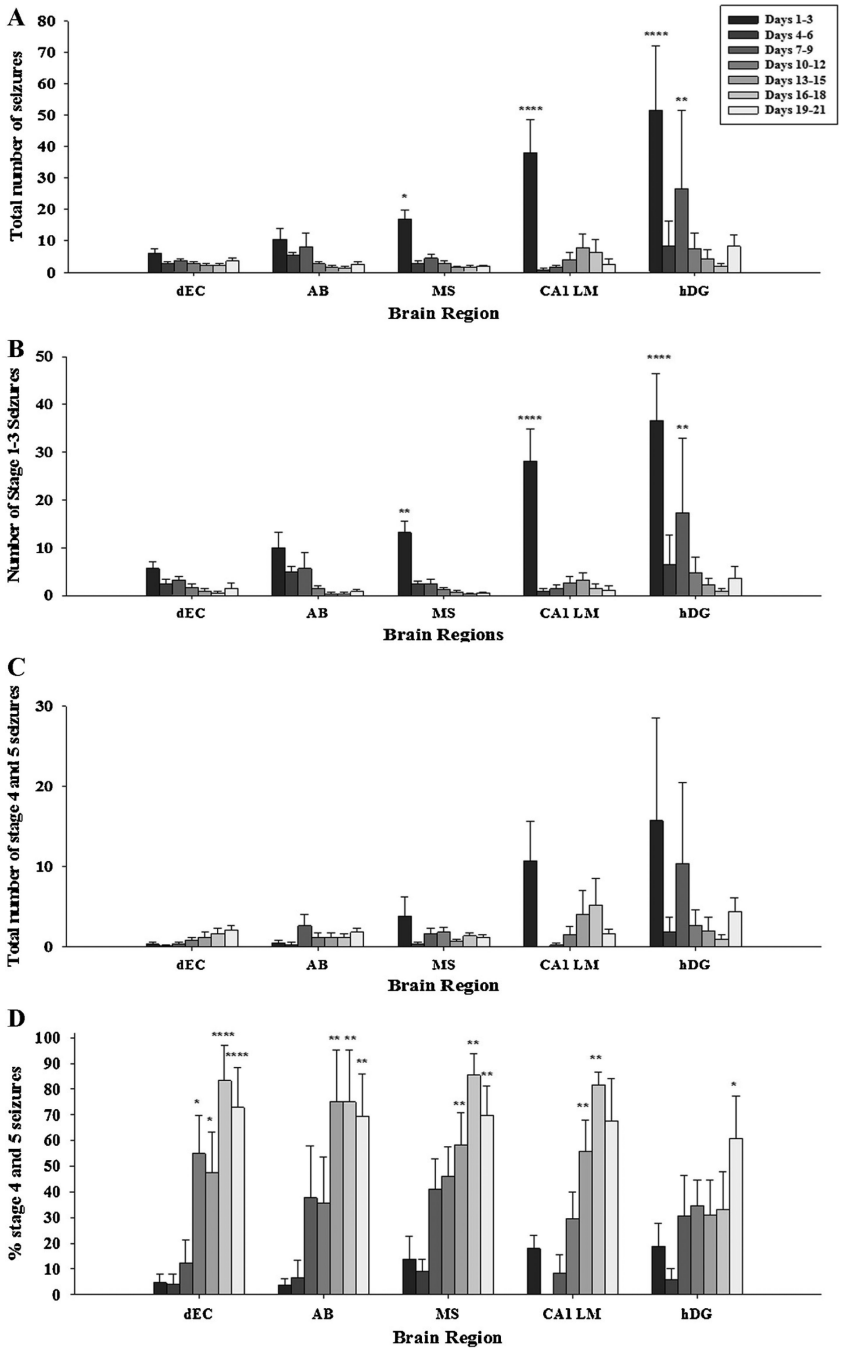

Figure 4.

(A) Effect of infusion site on seizure frequency binned over days 1–3, 4–6, 7–9, 10–12, 13–15, 16–18, 19–21; **** $p < 0.0001$ when compared to all groups with the exception of days 7–9 of the hilus of the dentate gyrus [hDG] group; ** $p < 0.01$ when compared to all groups with the exception of the CA1 lacunosum moleculare [CA1 LM], the molecular subiculum [MS], and the dentate gyrus groups on days 1–3; * $p < 0.05$ when compared to all other time points in that group. (B) Effect of infusion site on non-severe seizure type (Racine stages 1, 2, 3) of seizures over the first 21 days of MSO infusion. The number of stages 1–3 seizures

are shown for each infusion site and binned over days 1–3, 4–6, 7–9, 10–12, 13–15, 16–18, 19–21. **** $p < 0.0001$, *** $p < 0.001$, ** $p < 0.01$, when compared to all other time points for that group, with the exception of days 1–3 and days 7–9 of the dentate gyrus group. (C) Effect of infusion site on the number of most severe type (Racine stages 4 and 5) of seizures over the first 21 days of MSO infusion, binned over days 1–3, 4–6, 7–9, 10–12, 13–15, 16–18, 19–21; *** $p < 0.001$, * $p < 0.05$, when compared to all other time points for that group, with the exception of days 7–9 of the dentate gyrus group. (D) Effect of infusion site on the fraction (percent) of stages 4 and 5 seizures vs. all seizures are shown for each infusion site and binned over days 1–3, 4–6, 7–9, 10–12, 13–15, 16–18, 19–21; Abbreviations: Deep entorhinal cortex [dEC]; Angular bundle [AB]; **** $p < 0.0001$, *** $p < 0.001$, ** $p < 0.01$, * $p < 0.05$ when compared to their corresponding groups during days 1–3 and days 4–6. All values are provided as mean ± SEM.

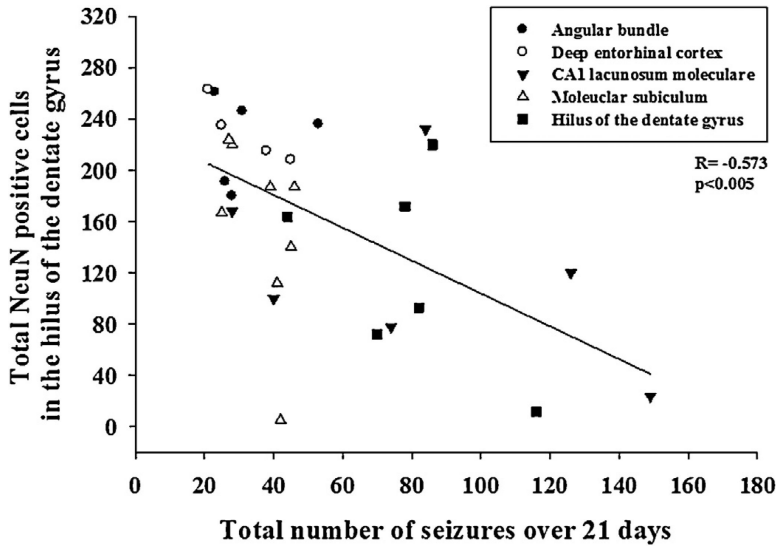

Figure 5.

Correlation between seizure frequency and neuronal loss in the hilus of the dentate gyrus. A significant negative correlation was found between the total number of seizures over 21 days and the total number of NeuN positive neurons in the hilus of the dentate gyrus ($R = -0.573$). Outliers have been excluded in the figure.

Abbreviations: Angular bundle [AB], Deep entorhinal cortex [dEC], CA1 lacunosum moleculare [CA1 LM], the molecular subiculum [MS], hilus of the dentate gyrus [hDG].